THE BUBBLE DISTRIBUTION IN GLASS REFINING CHANNELS

LUBOMÍR NĚMEC, PETRA CINCIBUSOVÁ

Laboratory of Inorganic Materials,
Joint Workplace of Institute of Inorganic Chemistry ASCR and Institute of Chemical Technology, Prague
Technická 5, 166 28 Prague 6, Czech Republic

E-mail: Lubomir.Nemec@vscht.cz

Submitted June 20, 2005; accepted September 26, 2005

Keywords: Glass fining, Bubble distribution models, Horizontal channel, Vertical channel

Equations were derived describing bubble distribution in horizontal, inclined and vertical channels with glass melt where bubbles behave as independent objects. The melt plug flow, as well as melt flow characterized by the parabolic velocity profile were considered in mentioned derivations. Using data typical for glass melting and fining, the bubble number and volume densities were calculated in a horizontal and vertical channels with downward plug flow. The bubble concentration profiles in the horizontal channel showed an almost permanent decrease of bubbles with time, while the vertical channel exhibited the bubble accumulation in the area where bubbles in downward flowing melt started to rise because of their growth. The concentration of bubbles in this area was at least by order of magnitude higher compared to bubble input concentration. This fact has both technological and theoretical consequences: coalescence should play a significant role in the accumulation area and convection currents could develop. The model considering the mutual influence of melt and bubbles should be applied.

INTRODUCTION

Different numerical models are used at present to reveal and describe melting processes with the aim to improve glass technology [1-9]. Nevertheless, their application for extensive parametrical studies faces frequently problems of longterm calculations and ambiguous interpretation of results acquired under real conditions. When searching for new concepts of the melting process, on the contrary, simple models valid under simplified conditions of the process may be very helpful. They frequently reveal more clearly the fundamental features of processes, facilitate extensive calculations and mark out the limits of simplified approaches [10]. This work will present the models of bubble distribution in channels with melt plug flow or with parabolical profile of flow velocity.

The mixture of glass melt and bubbles entering the refining channels is refined by bubble separation from the melt due to buyoancy force. Although another external forces or refining arrangement may be considered too, the separation in the gravitational field plays the crucial role up to present. The separation of bubbles according to Stokes´ law is significantly accelerated by mass transfer of dissolved gases from melt to bubbles. The sufficiently high temperature, lowered pressure and proper glass composition provides conditions for bubble growth by mentioned mass transfer. For a multicomponent bubble, the condition $\sum_i p_{imelt} \rangle p_{tot}$ is fulfilled where p_{imelt} are internal partial pressures of single gases in melt and p_{tot} is the total pressure inside the bubble. The refining gas considerably increases the sum of p_{imelt} at mentioned beneficial conditions. As is obvious from examination of the bubble separation process in spaces with different arrangement of glass flow patterns, the channels with parallel flow apear most convenient for rapid refining by bubble rising [11]. The critical features of the bubble separation process in refining channels may be investigated by description of single bubbles only, however, the bubble distribution in channels gives in some cases an instructive picture of the process or gives information about possible mutual influence of bubbles and melt. The goal of this work is to present relations making it possible to calculate the bubble distribution in mentioned channels and to present some results of bubble density calculations in the model horizontal and vertical channels.

CHANNELS WITH PLUG FLOW

The plug flow assumes an ideal fluid without friction, nevertheless, the bubble distribution in channels with plug flow gives an interesting qualitative information about process and forms a base for derivations of adequate relations in channels with real liquid. The analysis of separation of critical bubbles in different types of channels, namely horizontal, vertical and inclined, has shown that inclined channels do not provide special advantages for critical bubbles separation [11]. Despite that, the inclined channels will be treated in this work too. As bubbles in real melting process

reach the almost constant composition after relatively short time, so called stationary composition, all present bubbles will be considered stationary [12]. The important feature of stationary bubbles at constant temperature is almost linear growt with time. The bubble separation ability may be then at constant conditions characterized by the constant value of bubble growth rate, $\dot{a}$. The value of $\dot{a}$ is obtainable by laboratory measurements which fact ensures real validity of calculation results [13] .

Bubble distribution in an inclined channel with plug flow

The schematic picture of the inclined channel with entering bubbles is presented in figure 1. The initial number concentration of bubbles, expressed by the probability density function of the bubble size distribution, $f(a_o)$, is :

$$N_o = N_o \int_{a_{o\min}}^{a_{o\max}} f(a_o) da_o \qquad \left[numberm^{-3} \right] \tag{1}$$

where N_o is the initial bubble number density [number m^{-3}] and a_o is the initial bubble radius. The glass flows through the channel by the velocity v_{glass} and its layer in the channel has thickness h. The total concentration of bubbles in an arbitrary point of the channel should be calculated. The bubble velocity v_{bub} may be decomposed to the component perpendicular to the channel length l and parallel with channel length:

$$v_{bub}\perp = v_{bub}\cos\alpha \tag{2a}$$

$$v_{bub}|| = v_{bub}\sin\alpha \tag{2b}$$

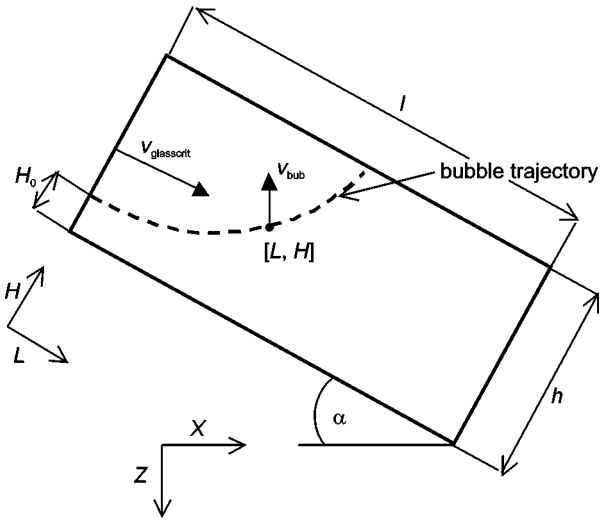

Figure 1. The scheme of the inclined opened channel. The horizontal channel emerges for $\alpha = 0$. [L,H] is the point where the bubble concentration is calculated.

The time necessary for the bubble with the initial radius a_{oi} to reach the point [L; H] is:

$$\tau_L = \frac{L}{v_{glasscrit}} \tag{3}$$

The value of $v_{glasscrit}$ represents the critical glass velocity. If glass melt flows with the critical velocity, the bubble of the minimum initial size, $a_{o\,\min}$, starting from the position $L = 0$, $H = 0$ reaches the glass level just at the end of the channel. The bubble velocity, $v_{bub}\perp$, is given by:

$$v_{bub}\perp = -\frac{2g\rho}{9\eta}\cos\alpha\left(a_o + \dot{a}\tau_l\right) \tag{4}$$

Taking into account that $\tau_l = l/v_{glasscrit}$ (see equation (3), for the bubble trajectory, h, perpendicular to the channel length, l, we have:

$$h = \frac{2g\rho}{9\eta}\cos\alpha\left[a_{o\min}^2\frac{l}{v_{glasscrit}} + a_{o\min}\dot{a}\left(\frac{l}{v_{glasscrit}}\right)^2 + \frac{\dot{a}^2}{3}\left(\frac{l}{v_{glasscrit}}\right)^3\right] \tag{5}$$

If $a_{o\,\min}$ is small enough, the members containing $a_{o\,\min}$ are neglected and:

$$v_{glasscrit} = 0.42\dot{a}^{2/3}l\left(\frac{g\rho\cos\alpha}{\eta h}\right)^{1/3} \tag{6}$$

If the bubble starts from the position H_o at $L = 0$, the distance perpendicular to l, H - H_o, should be run to reach the point [L; H]. The following equation is valid for linearly growing bubbles, analogically to (5):

$$H_o - H = \frac{2g\rho}{9\eta}\cos\alpha\left[a_o^2\frac{L}{v_{glasscrit}} + a_o\dot{a}\left(\frac{L}{v_{glasscrit}}\right)^2 + \frac{\dot{a}^2}{3}\left(\frac{L}{v_{glasscrit}}\right)^3\right] \tag{7}$$

The value of H_o is calculated from equation (7). For acceptable H_o holds that $H_o \in \langle 0; h\rangle$. If this condition is fulfilled, the bubble of the given size, a_o, is present in the point [L; H]. The total bubble number concentration in the point [L; H] is then the sum of all bubbles for which $H_o \in \langle 0; h\rangle$:

$$N[L;H] = N_o \int_{a'_{o\min}}^{a'_{o\max}} f(a_o) da_o \quad H_o \in \langle 0; h\rangle \tag{8}$$

where $a'_{o\,\min}$ and $a'_{o\,\max}$ are sizes of minimum and maximum bubbles crossing the point [L; H].

If the bubble volume concentration should be calculated, the bubble radius in any class of bubble sizes present in the point [L; H] is given by:

$$a = a_o + \dot{a}\frac{L}{v_{glasscrit}} \tag{9}$$

and the bubble volume concentration will be:

$$V_{bub} = 4/3\pi N_o \int_{a'_{o\min}}^{a'_{o\max}} f(a_o)\left(a_o + \dot{a}\frac{L}{v_{glasscrit}}\right)^3 da_o \quad [H_o \in \langle 0;h\rangle] \tag{10}$$

If channel is the horizontal one, $\alpha = 0$, $L = X$ and $H = Z$ (horizontal and vertical coordinates). Equation (7) emerges in the following form:

$$Z_o - Z = \frac{2g\rho}{9\eta}\left[a_o^2\frac{X}{v_{glasscrit}} + a_o\dot{a}\left(\frac{X}{v_{glasscrit}}\right)^2 + \frac{\dot{a}^2}{3}\left(\frac{X}{v_{glasscrit}}\right)^3\right] \tag{11}$$

where X and Z are coordinates of the given point in the channel.

Bubble distribution in a vertical channel with plug flow

Figure 2 presents situation in the vertical channel when glass and bubbles enter its upper part and flow downwards. Only the value of bubble velocity component parallel with the channel length, v_{bub} ||, plays role, i.e. $v_{bub} = v_{bub}$ ||. The bubble concentration in the point characterized by the Z coordinate, is calculated (see point [X; Z] in figure 2). In order to provide the complete bubble separation from melt, the bubbles in the smallest class of bubble sizes should reach the same absolute value of their rising velocity as is the melt descending velocity, $v_{glasscrit}$, just at the lower end of the channel, l:

$$|v_{bub\min}| = v_{glasscrit} = \frac{2g\rho}{9\eta}\left(a_{o\min} + \dot{a}\tau_l\right)^2 \tag{12}$$

where τ_l is time the smallest bubble needs to reach the inversion point Z‘ (see figure 2).

The value of $v_{glasscrit}$ ensuring refining of the smallest bubble is then calculated from equation:

$$dZ = \left[v_{glasscrit} - \frac{2g\rho}{9\eta}\left(a_{o\min} + \dot{a}\tau\right)^2\right]d\tau \tag{13}$$

and:

$$\int_0^l dZ = l = v_{glasscrit}\tau_l - \frac{2g\rho}{9\eta}\left(a_{o\min}^2\tau_l + a_{o\min}\dot{a}\tau_l^2 + \frac{\dot{a}^2\tau_l^3}{3}\right) \tag{14}$$

Equation (12) is valid for $v_{glasscrit}$, after substitution of equation (12) into (14) and rearrangement, we get:

$$l = \frac{2g\rho}{9\eta}\left(a_{o\min}\dot{a}\tau_l^2 + 2/3\dot{a}^2\tau_l^3\right) \tag{15}$$

For the growing bubble of initial minimum size, $a_{o\,\min}$, and in later stages of the bubble separation, we can neglect the first term in parentheses of equation (15) (for $a_{o\,\min} = 5\times10^{-5}$ m, $\dot{a} = 1\times10^{-7}$ m, $\tau_R = 1\times10^4$ s, the error by neglecting $a_{o\,\min}$ is less than 10 %, g.e.) and:

$$\tau_l = \left(\frac{27\eta l}{4g\rho\dot{a}^2}\right)^{1/3} \tag{16}$$

The value of maximum admitted glass velocity, $v_{glasscrit}$, after substituting equation (16) into (12), is given by:

$$v_{glasscrit} = 0.794\dot{a}^{2/3}l^{2/3}\left(\frac{g\rho}{\eta}\right)^{1/3} \tag{17}$$

When calculating the bubble concentrations in an arbitrary point of the channel, the downward and upward movement of bubbles must be taken into account. Thus, every bubble which met the given point [X; Z] during its downwardt trajectory, shoud meet it as well when subsequently rises to the level. As bubbles in the vertical channel are neither lost nor accumulated, the bubble number density balance of every bubble size at any horizontal level is valid in the steady state:

$$dN_o S\left[v_{glasscrit} - v_{bubo}(\tau = 0, Z = 0)\right] = dN_Z S\left[v_{glasscrit} - v_{bubZ}\right] \tag{18}$$

where N_Z is the number density of bubbles crossing the point [X; Z], S is the cross section of the channel (here constant with Z), v_{bubo} is the initial bubble rising velocity and v_{bubZ} is the bubble rising velocity in the point [X; Z]. For N_Z is valid:

$$N_Z = N_o \int_{a'_{o\min}}^{a'_{o\max}} f(a_o)\frac{v_{glasscrit} - v_{bubo}}{v_{glasscrit} - v_{bubZ}} da_o \tag{19}$$

where $a'_{o\,\min}$ and $a'_{o\,\max}$ are the minimum and maximum bubbles crossing the point [X; Z].

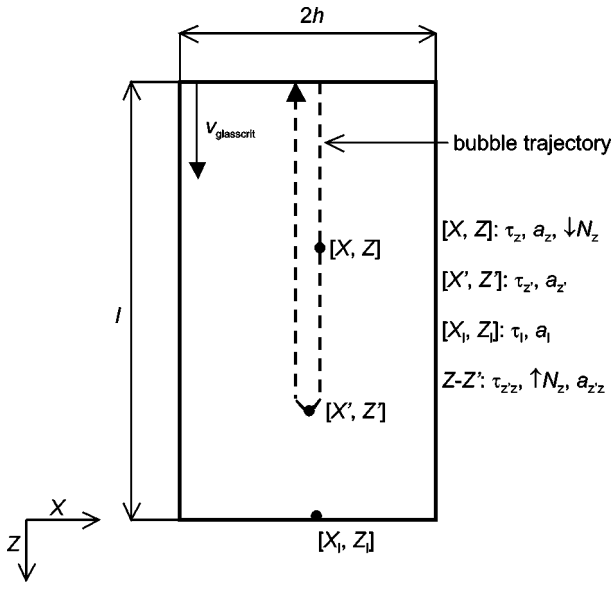

Figure 2. The scheme of the vertical channel. [X, Z] is the point where the total bubble concentration is calculated. [X', Z'] is the bubble inversion point, [X_l, Z_l] is the inversion point of the critical (smallest) bubble.

Bubbles in downward flow

Analogically to equation (14), we get for the bubble trajectory in Z (see figure 2):

$$Z = v_{glasscrit}\tau_Z - \frac{2g\rho}{9\eta}\left(a_o^2\tau_Z + a_o\dot{a}\tau_Z^2 + \frac{\dot{a}^2\tau_Z^3}{3}\right) \qquad (20)$$

The value of τ_Z is calculated from equation (20) and for the bubble rising velocity in the point Z holds:

$$v_{bubZ} = -\frac{2g\rho}{9\eta}\left[a_o + \dot{a}\tau_Z\right]^2 \qquad (21)$$

τ_Z is obtained from equation (20).

The bubble number density of descending bubbles, $\downarrow N_Z$, in the point [X; Z] is therefore:

$$\downarrow N_Z = N_o \int_{a'_{o\min}}^{a'_{o\max}} \frac{v_{glasscrit} - \frac{2g\rho}{9\eta}a_o^2}{v_{glasscrit} - \frac{2g\rho}{9\eta}\left(a_o + \dot{a}\tau_Z\right)^2} f\left(a_o\right)da_o \qquad (22)$$

The bubble volume concentration in the point [X; Z] is then given by:

$$V_{bub} = 4/3\pi N_o \int_{a'_{o\min}}^{a'_{o\max}} \frac{v_{glasscrit} - 2g\rho a_o^2/9\eta}{v_{glasscrit} - 2g\rho\left(a_o + \dot{a}\tau_Z\right)^2/9\eta}\left(a_o + \dot{a}\tau_Z\right)^3 f\left(a_o\right)da_o \qquad (23)$$

From equation (22) results that bubble concentration in the downflowing glass melt will grow. If, on the contrary, the melt with bubbles would enter the space from the lower end of the channel, the bubble number concentration would decrease with decrasing bubble depth under glass level. The both signs minus in equation (22) should be then replaced by plus.

The bubble density remains constant for bubbles of constant size ($\dot{a} = 0$).

Bubbles in upward flow

Primarily the bubble parameters in the inversion point [X'; Z'] in figure 2 are to be calculated. For time necessary to reach the inversion point Z', equation (17) is valid, defining $v_{glasscrit}$. $v_{glasscrit}$ should have the same absolute value as the bubble rising velocity in the point Z':

$$0.794\dot{a}^{2/3}l^{2/3}\left(\frac{g\rho}{\eta}\right)^{1/3} = \frac{2g\rho}{9\eta}\left(a_o + \dot{a}\tau_{Z'}\right)^2 \qquad (24)$$

after arrangement:

$$\tau_{Z'} = 1.89\left(\frac{\eta l}{g\rho\dot{a}^2}\right)^{1/3} - \frac{a_o}{\dot{a}} \qquad (25)$$

and the value of $a_{Z'}$ is calculated from:

$$a_{Z'} = a_o + \dot{a}\tau_{Z'} \qquad (26)$$

The bubbles rising from the point [X'; Z'] should further get over the distance Z' - Z to meet the point [X; Z] again. The time $\tau_{Z'Z}$ needed is calculated from:

$$Z - Z' = v_{glasscrit}\tau_{Z'Z} - \frac{2g\rho}{9\eta}\left(a_{Z'}^2\tau_{Z'Z} + a_{Z'}\dot{a}\tau_{Z'Z}^2 + \frac{\dot{a}^2}{3}\tau_{Z'Z}^3\right) \qquad (27)$$

and the concentration of ascending bubbles in the point [X; Z], $\uparrow N_Z$, is given by equation:

$$\uparrow N_Z = N_o \int_{a'_{o\min}}^{a'_{o\max}} \frac{v_{glasscrit} - \frac{2g\rho}{9\eta}a_o^2}{\frac{2g\rho}{9\eta}\left(a_{Z'} + \dot{a}\tau_{Z'Z}\right)^2 - v_{glasscrit}} f\left(a_o\right)da_o \qquad (28)$$

Equation analogical to equation (23) but with the appropriate values of $a_{Z'}$ instead of a_o and $\tau_{Z'Z}$ instead of τ_Z in the denominator and behind the fraction on the right side of this equation is valid for the relative volume of bubbles, $\uparrow V_{bub}$. The signs of velocities in the denominator should be changed too.

Notice that theoretically $N \to \infty$ in the inversion point as $v_{glasscrit} = v_{bub}$ (denominator of equation (28)). The calculation of bubble concentrations just in inversion points does not however physical meaning as bubbles do not form a genuine continuum. The maximum bubble concentrations may be calculated only in the proximity of the inversion point. In this procedure, the average vertical distance between bubbles of the same class of bubble sizes is calculated. If the initial number of bubbles in the i-th class of bubble sizes is N_{oi}, then the initial average distance between bubbles, l_{oi}, is given by:

$$l_{oi} = \frac{1}{N_{oi}^{1/3}} \quad [\mathrm{m}] \qquad (29)$$

and the time period between two bubbles entering the channel is:

$$\tau_i = \frac{l_{oi}}{v_{glasscrit} - \frac{2g\rho}{9\eta}a_{oi}^2} \qquad (30)$$

The vertical distance between two subsequent bubbles, one of them being in the inversion point, is:

$$l_{iZ'} = Z' - v_{glasscrit}\left(\tau_{Z'} - \tau_i\right) + \frac{2g\rho}{9\eta}\left[a_{oi}^2\left(\tau_{Z'} - \tau_i\right) + a_{oi}\dot{a}\left(\tau_{Z'} - \tau_i\right)^2 + \frac{\dot{a}^2}{3}\left(\tau_{Z'} - \tau_i\right)^3\right] \qquad (31)$$

and for the bubble number density in the point [X; Z] is valid:

$$N_{Z'} = \frac{l_{oi}}{l_{iZ'}} N_{oi} \tag{32}$$

The total concentration of bubbles (descending and ascending bubbles) in the point [X; Z] is then given by:

$$N_Z = \downarrow N_Z + \uparrow N_Z \tag{34}$$

where $\downarrow N_Z$ is given by equation (22) and $\uparrow N_Z$ by equation (28).

Similarly V_Z is determined by the sum of values calculated from equations (23) and from its appropriate form for ascending bubbles (see the text behind equation (28)).

CHANNELS WITH PARABOLIC VELOCITY PROFILE

The opened inclined channels were considered for small channel inclinations and the closed channels were taken into account for channels with great inclination angels to calculate the bubble concentration field. The central longitudinal or vertical section through channels was considered as the critical one.

Horizontal channel

As in the case of channels with plug flow, the starting position of bubbles going through the given point is sought for. The bubble moving in the critical central longitudinal section through the channel has to pass through the distance H_o - H. For the longitudinal distance L of the given point, we have the equation [11]:

$$L = v_{glasscrit}\tau_L - \frac{v_{glasscrit}}{h^2}\int_0^{\tau_L}\left[h - H_o - \frac{2g\rho}{9\eta}\cos\alpha\left(a_o^2\tau + a_o\dot{a}\tau^2 + \frac{\dot{a}^2\tau^3}{3}\right)\right]^2 d\tau \tag{35}$$

and for the vertical distance H_o - H holds:

$$H_o - H = \frac{2g\rho}{9\eta}\cos\alpha\left[a_o^2\tau_L + a_o\tau_L^2 + \frac{\dot{a}^2\tau_L^3}{3}\right] \tag{36}$$

The values H_o and τ_L are obtained by simultaneous solution of equations (35-36). In case of the horizontal channel ($\alpha = 0$), the $\cos\alpha = 1$ and coordinates X and Z are substituted into equations (35-36) instead of L and H. Values of H_o (Z_o) $\in \langle 0; h\rangle$ are acceptable for opened channels (horizontal channels or channels with low inclination angle α and values $H_o \in \langle 0; 2h\rangle$ for closed channels with high inclination angle (see figures 1 and 2). In order to calculate the bubble number density in the given point [L; H], equation (8) is applied. For the calculation of bubble volume concentration, equation (10) is applied.

The value:

$$a_L = a_o + \dot{a}\tau_L \tag{37}$$

is substituted into parentheses on the right side of equation (10).

The value of $v_{glasscrit}$ should be acquired from the critical trajectory of minimum bubble through the channel. According to [11], the average critical glass velocity in the opened horizontal channel may be calculated from the equation:

$$l = 3.18\bar{v}\left(\frac{\eta h}{g\rho\dot{a}^2}\right)^{1/3} \tag{38}$$

where $\bar{v}$ is the average glass velocity in the channel.

The equality $v_{glasscrit} = 2\bar{v}$ is valid for the circular channel while equality $v_{glasscrit} = 2.25\bar{v}$ holds for the rectangular channel.

Vertical channel

The glass velocity distribution in the vertical channel is given by the equation (see figure 2):

$$v_{glass} = v_{glasscrit} - \frac{v_{glasscrit}}{h^2}(h - X)^2 \tag{39}$$

here, the critical trajectory is at h and the critical average glass velocity can be calculated from the equation:

$$l = 4.0\bar{v}_{glass}^{3/2}\left(\frac{\eta}{g\rho\dot{a}^2}\right)^{1/2} \tag{40}$$

as in the previous case, $v_{glasscrit} = 2\bar{v}_{glass}$ for the circular channel and $v_{glasscrit} = 2.25\bar{v}_{glass}$ for the rectangular one.

When calculating the bubble distribution in the vertical channel, the value of v_{glass} from equation (39) is used in equations instead of $v_{glasscrit}$ in equations (20-28). The same value of v_{glass} is substituted on the left side of equation (24).

RESULTS OF MODEL CALCULATIONS AND DISCUSSION

The horizontal and vertical channels with plug flow were chosen for calculations. The aim of these calculations was to ascertain average concentrations and bubble distributions in both kinds of channels for a typical case of refining. When searching for new refining principles, frequently only critical bubbles are followed, regardless to possible impact of bubble multitude on glass flow and glass properties. The calculations of bubble fields may provide justification of the proposed simplified picture of the refining problem. Some results may contribute to correct qualitative image of bubble behavior and overall impact on melting under real conditions without application of relatively complicated numerical models.

When calculating the channels, its sizes according to figures 1 and 2 were: l = 1 m, h = 0.5 m, w (channel width) = 0.5 m. Only concentrations in the central section of channels were calculated as the central sections are critical. The glass density was 2300 kg/m^3, its viscosity 20 Pas, the bubble growth rate $\dot{a}$ was 5×10^{-7} m/s.

The horizontal channel with plug flow

The initial radius of entering bubbles was: $a_o \in \langle 5\times10^{-5}; 5\times10^{-4}\ \mathrm{m}\rangle$. The bubbles of arbitrary size had the same representation, thus: $f(a_o)$ = const, $N_o = 5\times10^6$ bubbles per m^3. In the given case, the value of $f(a_o)$ was 2222 m^{-1} and the value of $v_{glasscrit}$ according to equation (6) was 3.595×10^{-4} m/s. Figure 3 presents the trajectories of two bubbles in the channel having the border values, namely $a_o = 5\times10^{-5}$ and 5×10^{-4} m. In the area below the curve $a_0 = 5\times10^{-5}$ m will be no bubbles, while in the area above $a_o = 5\times10^{-4}$ m will be all entering bubbles. The area between both curves is characterized by changing both number and volume density of bubbles. The vertical bubble variations are brought about by bubble removing due to their rising. Figure 4 brings the vertical concentration profiles of bubble number densities at X = 0 (N = const = 5×10^6 m^{-3}); 0.2; 0.4; 0.6; 0.8 and 0.9 m, calculated according to equation (8). The bubble number densities decrease both with growing X and Z owing to bubble separation in the region between both curves from figure 3. The appropriate bubble volume densities in vertical profiles are presented in figure 6 in the ln form. The bubble volume densities provide a similar picture as bubble number densities presented in fi-gure 4, the relative bubble volume densities increased however with increasing X and constant Z owing to bubble growth with time. While the standard value of inputting bubbles was 0.0728 vol.%, the maximum value at X = 0.6-0.8 m and on the glass level attained 2.98 vol.% due to bubble growth. This is demonstrated by logarithmical curves in figure 5 where the bubble volume densities are plotted against X coordinate for Z = 0, Z = 0.125 and Z = 0.35 m. The bubble number densities for Z = 0 are plotted too. Because higher bubble densities are set up close to the glass level, the melt is stabilized with respect to the vertical density gradient. The maxima on dependences between bubble volume densities and X coordinate obvious in figure 5 may however evoke two circulation flows with upward current in the region of maxima. The maxima are result of two effects: increasing single bubble volume due to bubble growth and decreasing bubble number due to bubble rising to the level. It is believed that apparent glass convection may be expected at slightly higher bubble concentrations than in the presented case.

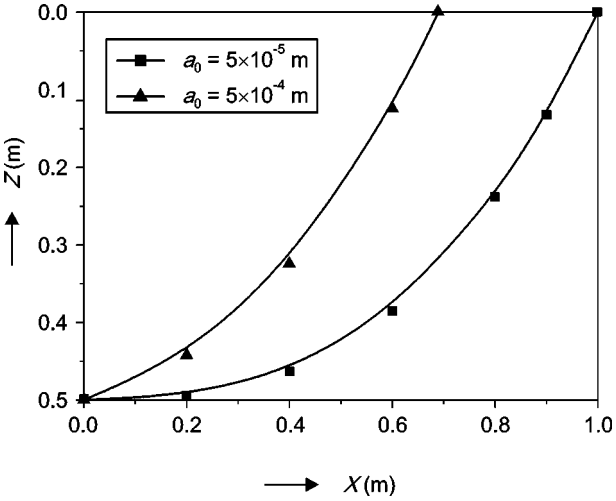

Figure 3. The pathways of bubbles with minimum and maximum sizes in the horizontal channel with plug flow.

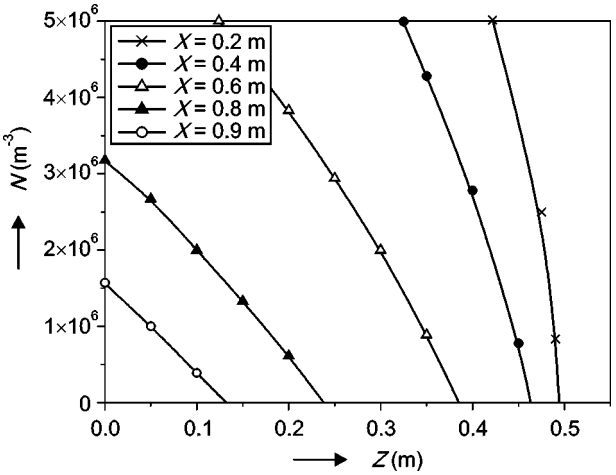

Figure 4. The vertical profiles of the bubble number densities in the horizontal channel with plug flow.

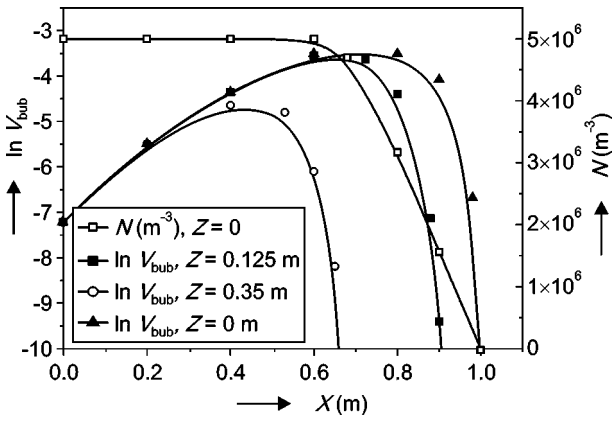

Figure 5. The horizontal profiles of the bubble number density at Z = 0 and the bubble volume densities at Z = 0, Z = 0.125 and Z = 0.35 m.

The vertical channel with plug flow

The interesting picture provide vertical concentration profiles of monodisperze bubles as presents figures 7 and 8. The class of minimum bubble sizes, $\bar{a}_o = 5\times10^{-5}$ m, and maximum bubble sizes, $\bar{a}_o = 5\times10^{-4}$ m, were elected for the presentation of bubble number densities versus vertical coordinate Z. The bubble number concentration of down flowing bubbles grows with Z because bubbles move against glass melt low (see equation (22) and reaches an extremely high value approximately 1.4×10^8 bubbles/m^3 in the inversion point Z' (the value is independent from a_o) according to equations (29-32). The bubble number density decreases, on the contrary, for rising bubbles (with decreasing Z), as is as well obvious from both figures 7 and 8 and results from equation (28). The entire bubble number density exhibits then a distinct increase with growing depth below glass level and reaches its maximum in the inversion point (see figures 7 and 8). From the nature of bubble kinetics further results that bubble sizes in the inversion point are independent from the initial bubble size and depend only on the value of v_{glass} or $v_{glasscrit}$. The numbers and volumes of bubbles in the inversion point are as well independent from a_o. The monodisperze bubble files are however rare, in fact the continual spectrum of bubble sizes should be expected and much lower bubble densities close to bubble inversion points may be expected.

In following figures are therefore plotted average bubble concentrations calculated in horizontal layers with different vertical thickness (the thickness decreases towards to the inversion point). Figure 9 presents the average concentrations of downstreaming and rising bubbles, as well as the total bubble number densities in horizontal layers for bubbles in the size class $a_o = 5\times10^{-5}$ m. The single curves are only guidance for eyes. The total bubble number densities of monodisperze bubbles in the given point for $a_o = 5\times10^{-5}$ m are as well plotted for comparison. With the exception of the inversion point, the average concentrations are well comparable both by the character of dependence and values of bubble concentrations with concentrations of monodisperze bubbles in single points. The average value of the total bubble number density in the layer close to the inversion point (the thickness of the layer is 0.01 m) is still about 2.7×10^7 bubbles per m^3, i.e more than one order of magnitude higher compared to initial bubble number density 1×10^6 bubbles per m^3. The similar character exhibit the number densities of remaining bubble size classes as is altogether presented in figure 10. The figure shows that concentrations of bubbles steeply grow in the area of bubble inversion points, i.e. between 0.5 - 1 m. The bubble number densities close to inversion point are only slightly dependent on the initial bubble size and move between 2.3 - 2.7×10^7 bubbles per m^3.

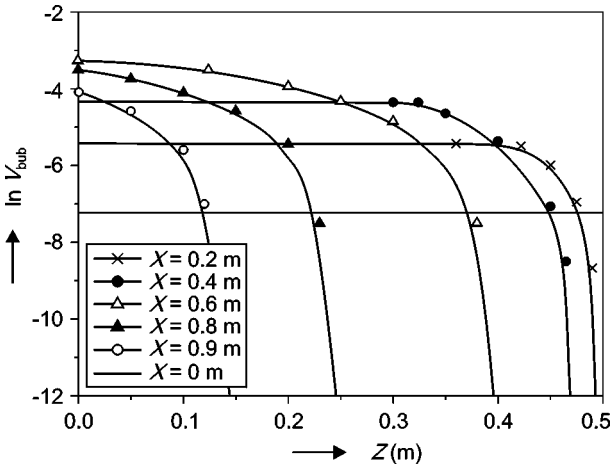

Figure 6. The vertical profiles of the bubble volume density in the horizontal channel with plug flow.

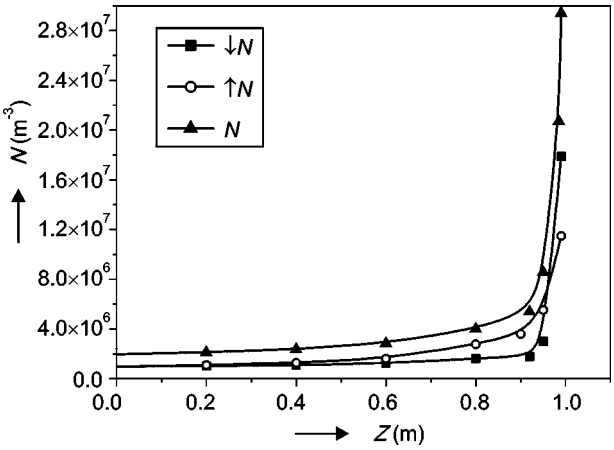

Figure 7. The vertical profile of the bubble number density in the vertical channel with plug flow for monodisperze bubbles, $a_o = 5\times10^{-5}$ m. ↓N - downstreaming bubbles, ↑N - upstreaming bubbles, N - the total bubble concentration.

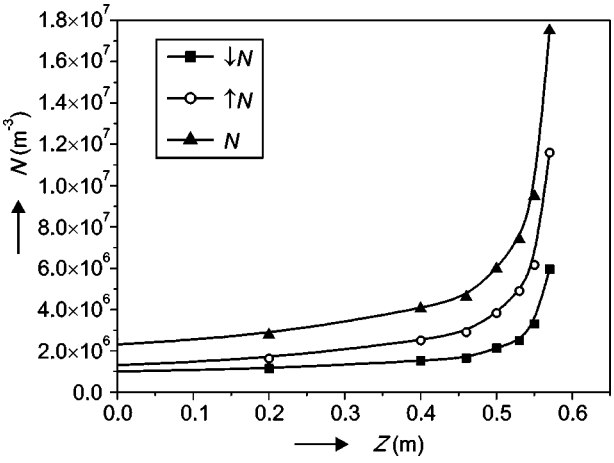

Figure 8. The vertical profile of the bubble number density in the vertical channel with plug flow for monodisperze bubbles, $a_o = 4.5\times10^{-4}$ m. ↓N - downstreaming bubbles, ↑N - upstreaming bubbles, N - the total bubble concentration.

The bubble volume concentrations are nevertheless the more instructive information about bubble potential impact on melt behavior. The average bubble volume densities for five bubble size classes are plotted in figure 11. The concentrations of gas phase in the melt are distinctly greater than 20 vol.% in the area of inversion points (the average bubble volume concentration very close to the inversion point is even more than 30 vol. %). The overall average volume densities of bubbles are plotted in figure 12 and confirm the fact that bubble concentration steeply increases in the region of bubble inversion points. The mentioned fact should have decisive consequences for behavior of both bubbles and melt in this region. The bubble coalescence should play an important role for bubble removing, the high concentrations of bubbles should evoke flow instability resulting in intensive convective currents. The presented model of single bubbles may be therefore valid only for very low bubble input concentrations. The presented facts have practical significance for the fining process in vertical furnaces with electric heating. The high bubble concentrations, bubble coalescence and intensive convective currents evoked by bubbles may be expected in fining zones. The more sophisticated numerical models, taking into account the mutual influence of bubbles and melt, should be then applied [14].

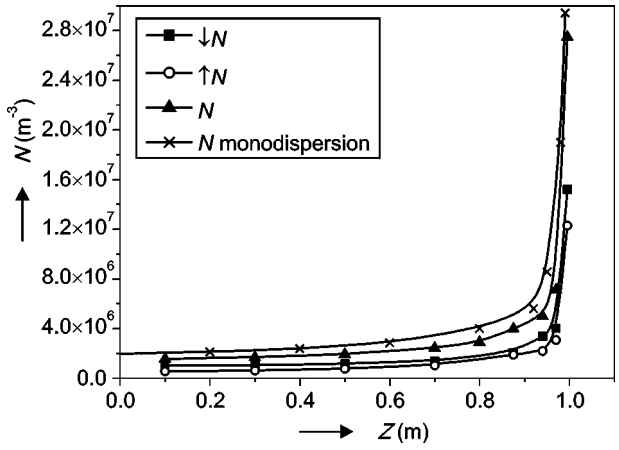

Figure 9. The dependence between average bubble number densities and the vertical coordinate in the vertical channel with plug flow. $a_o = 5\times10^{-5}$ m. The lines are only guidance for eyes. $\downarrow N$ - downstreaming bubbles, $\uparrow N$ - upstreaming bubbles, N - the total bubble concentration.

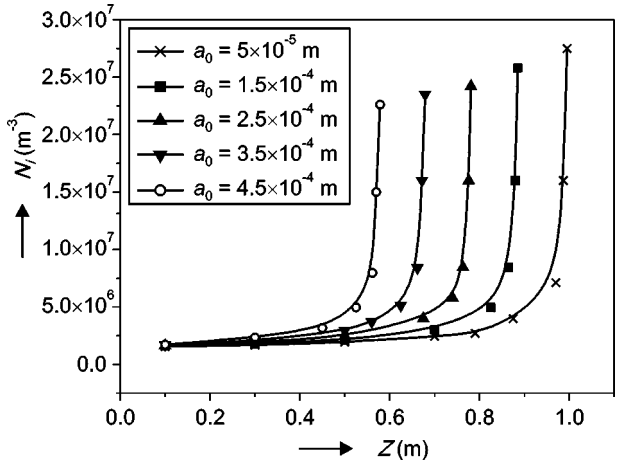

Figure 10. The overall view of the dependence between average bubble number densities and the vertical coordinate in the vertical channel with plug flow. The lines are only guidance for eyes.

CONCLUSIONS

The presented models give information about justification of using the very simple models neglecting mutual independence of bubbles and melt during bubble separation process. If such model is valid, only s.c. critical bubbles may be used for evaluation of refining abi-

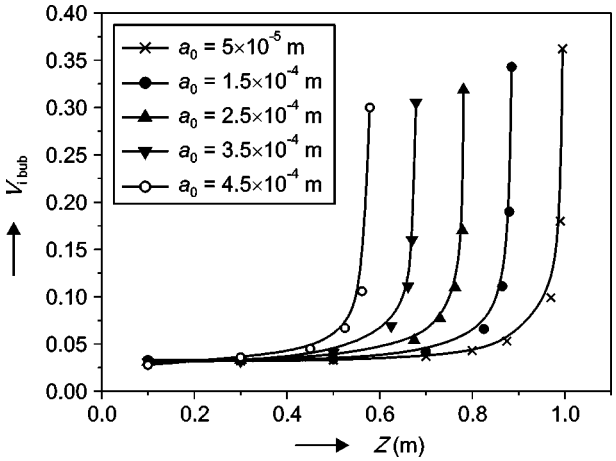

Figure 11. The overall view of the dependence between average bubble volume densities and the vertical coordinate in the vertical channel with plug flow. The lines are only guidance for eyes.

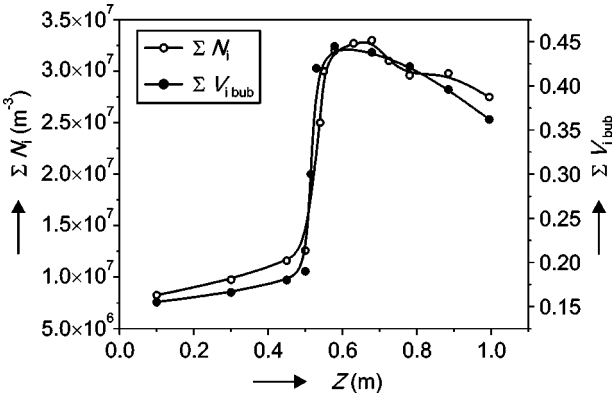

Figure 12. The dependence between total average bubble concentrations and the vertical coordinate in the vertical channel with plug flow. The lines are only guidance for eyes.

lity of simple glass melting spaces. This fact is particularly significant when searching for new concepts and conditions of the bubble separation process. The results published in this work have shown, that the almost independent behavior of bubbles and melt can be expected in horizontal channels where the bubble concentrations integrally decrease with time. At higher bubble concentrations, however, the maxima of bubble volume densities versus X coordinate may bring about convection currents with upward flow in the region of mentioned maxima. In vertical channels, the accumulation of bubbles occurs in the area where most of bubbles reach the same absolute value of their rising velocity as is the local melt downward velocity (inversion point). The high bubble concentrations in this area should lead to bubble coalescence and concentration convection of the melt. The more complex models have to be therefore used for description of the process. Nevertheless, the presented model provided a fundamental qualitative information about fining process in vertical electrical furnaces. It can be used for vertical channels with low bubble input concentration.

Acknowledgement

This work was supported in the framework of the Institutional Research Plan No.Z40320502 entitled Design, synthesis and characterisation of clusters, composites, complexes and other compounds based on inorganic substances; mechanisms and kinetics of their interactions.

References

1. Kramer F. in: *Gas bubbles in glass*, International Commission on Glass, p.92, 1985.
2. Kramer F.: Glastechn.Ber. *52*, 43 (1979).
3. Němec L.: Glass Technol. *21*, 134 (1980).
4. Onorato P. I. K., Weinberg M. C., Uhlmann D. R.: J.Am.Ceram.Soc. *64*, 676 (1981).
5. Ramos J. I.: J.Am.Ceram.Soc. *69*, 149 (1986).
6. Itoh E., Yoshikawa H., Kawase Y: Glastechn.Ber.Glass Sci.Technol. *70*, 8 (1997).
7. Kawachi S., Kawase Y.: Glastechn.Ber.Glass Sci.Technol. *71*, 83 (1998).
8. Beerkens R. C. G.: Glastechn.Ber.Sonderband *63K*, 222 (1990).
9. Beerkens R. C. G: *Advanced Fusion and Processing of Glass*, July 27-30, 2003, Rochester NY USA, p. 1.
10. Kloužek J., Němec L., Ullrich J.: Glastechn.Ber.Glass Sci.Technol. *73*, 329 (2000).
11. Němec L., Jebavá M., Tonarová V. : *Proceedings of the VIII International Seminar on Mathematical Modeling and Advanced Numerical Methods in Furnace Design and Operation*, May 19-20, 2005, Velké Karlovice, CR, p. 24.
12. Němec L., Muhlbauer M.: Glastechn.Ber. *54*, 99 (1981).
13. Jebavá M., Němec L., Kloužek J.: Ceramics-Silikáty *48*, 121 (2004).
14. Matyáš J., Němec L.: Glass Sci.Technol. *76*, 71 (2003).

DISTRIBUCE BUBLIN V KANÁLECH SE SKELNOU TAVENINOU

LUBOMÍR NĚMEC, PETRA CINCIBUSOVÁ

Laboratoř anorganických materiálů
Společné pracoviště Ústavu anorganické chemie AVČR
a Vysoké školy chemicko-technologické v Praze
Technická 5, 166 28 Praha 6

Byly odvozeny rovnice popisující distribuci bublin v nakloněných, horizontálních a vertikálních kanálech se skelnou taveninou charakterizovanou pístovým tokem nebo tokem s parabolickým profilem rychlostí. Bubliny se chovaly jako nezávislé objekty. S použitím dat typických pro separaci bublin ve skelných taveninách při tavicím procesu skel byly vypočteny distribuce bublin v ustáleném stavu v horizontálním a vertikálním kanále s pístovým tokem. Výsledky výpočtů ukázaly, že v horizontálních kanálech dochází prakticky v celém horizontálním profilu k úbytku počtu bublin jejich výstupem, zatímco objemový podíl bublin tvoří maxima; při vysokých vstupních koncentracích bublin se pak může objevit konvekční proudění. Ve vertikálním kanále dochází k akumulaci bublin v oblasti, kde rostoucí bubliny klesající nejprve s proudem skloviny začínají stoupat k hladině. Koncentrace bublin v této oblasti stoupne nejméně o řád oproti koncentraci vstupní. Vzrůst koncentrací má technologické i teoretické důsledky: v oblasti vysokých koncentrací bublin se patrně významně uplatní jejich koalescence a vznikne výrazné konvekční proudění i při relativně nízkých vstupních koncentracích bublin. Pro popis koncentračních polí bublin ve vertikálních kanálech s běžnými koncentracemi vstupujících bublin je proto většinou třeba použít modelů uvažujících vzájemný vliv bublin a taveniny.